

Magnetohydrodynamic Stokes Problem for a Dissipative Heat Generating Fluid with Hall and Ion-slip Currents, Mass diffusion and Radiation Absorption

J. K. Kwanza, M. Kinyanjui and S. M. Uppal

Mathematics Department, Jomo Kenyatta University of Agriculture and Technology, P.O Box 62000, NAIROBI ,KENYA
E-mail: kwanzakioko@yahoo.com

ABSTRACT

Heat and Mass transfer MHD stokes problem for a dissipative heat generating fluid with radiation absorption, mass diffusion, Hall and ion-slip currents is presented. The set of governing equations for the problem are solved by a finite difference algorithm. Effects of the various parameters in the laminar boundary layer on concentration, rate of mass transfer, velocity, skin friction, temperature and rate of heat transfer are discussed with the aid of graphs and tables.

KEY WORDS: Ion-slip current, Hall current, Radiation Absorption, Mass transfer, Heat transfer, Magnetic field, Dissipative heat, Free convection.

NOMENCLATURE

SYMBOL QUANTITY

C_p	Specific heat at constant pressure, j/kgK
C	Dimensionless concentration of the injected material
C^+	Dimensional concentration of the injected material, kg/m ³
C_w^+	Concentration of the injected material at the plate, kg/m ³
C_∞^+	Concentration of the injected material in the free stream, kg/m ³
D	Diffusion coefficient, m ² /s
E_c	Eckert number
E	Electric field, volt/m
e	Electric charge coul./m ³
g	Acceleration due to gravity
G_c	Modified grashof number
Gr	Grashof number
H	Magnetic field intensity, weber/m ²
J	Current density, A/m ²

j_x^+, j_y^+, j_z^+	Components of current density, JA/m^2
k	Thermal conductivity, $\text{w}/\text{m}\cdot\text{k}$
M	Magnetic parameter
m	Hall parameter
n	Ion-slip current parameter
N_u	Nusselt number
P_r	Prandtl number
P_e	The electron pressure, N/m^2
Q_1^+	Coefficient of proportionality for absorption of radiation, $\text{w}/\text{m}^3\cdot\text{k}$
Q^+	Internal heat generation, w/m^3
Sh	Sherwood number
Sc	Schmidt number
t	Dimensionless time, s
t^+	Dimensional time, s
T^+	Dimensional temperature of the fluid, k
T_∞^+	Temperature of the fluid in the free stream, k
T_w^+	Temperature of the plate, k
u^+, v^+, w^+	Velocity components, m/s
ν_c	Electron-atom collision frequency
u_o^+	Suction velocity, m/s
u_o	Dimensionless suction velocity
x^+, y^+, z^+	Cartesian co-ordinates, m

GREEK SYMBOLS

θ	Dimensional temperature of the fluid
δ	Heat source parameter
ω	Cyclotron frequency, Hz
ω_e	Electron cyclotron frequency, Hz
ω_i	Ion cyclotron frequency, Hz
μ_e	Magnetic permeability, Hm^{-1}
ρ	Fluid density, kg/m^3

η_e	Number density of electrons
ν	Kinematic viscosity, m^2/s
β	Coefficient of volumetric expansion, k^{-1}
β^*	Coefficient of volumetric expansion due to concentration gradients, k^{-1}
τ_e	Collision time of electrons, s
τ_i	Collision time of ions, s
σ	Electrical conductivity, $\Omega^{-1}m^{-1}$
τ_y	Skin friction due to primary velocity profile
τ_z	Skin friction due to secondary velocity profile

1.0 INTRODUCTION

The phenomenon of heat and mass transfer coupled with radiation absorption in magnetohydrodynamics is important due to its applications in astrophysics, geophysics and engineering Schercliff (1965). The subject became popular in 1950s when the importance of controlled fusion research and that of space technology became evident. Since then extensive literature has been published in journals and reports. Bansal et al (1987) investigated magnetofluiddynamic boundary layer flow in the presence of transverse magnetic field. They studied the effects of magnetic field on skin friction and heat transfer rate. Dash and Ojha (1991) presented their study on magnetohydrodynamic unsteady free convection effect on the flow past an exponentially accelerated vertical plate. Hall effects on hydromagnetic free convection flow along a porous flat plate with mass transfer was investigated by Hossein and Rashid (1987). Chaturvedi studied the flow past a uniformly started porous plate with constant suction. Ram (1991) used a finite difference method to analyse the MHD stoke's problem for a vertical plate with Hall and ion-slip currents. Coupled heat and mass transfer by natural convection from a horizontal line source in a saturated porous medium was presented by Lai (1990). Convection heat and mass transfer of a viscous flow past a hot vertical plane wall with periodic suction and heat sources was investigated by Dash and Tripathy. Kinyanjui et al (1998) studied stokes problem for a vertical infinite plate in a dissipative rotating fluid with hall current. Recently, Kinyanjui et al (2001) presented MHD free convection heat and mass transfer of a heat generating fluid past an impulsively started infinite vertical porous plate with hall current and Radiation absorption.

Despite the studies outlined above, the problem of MHD boundary layer flow of a viscous incompressible heat generating fluid past an infinite vertical porous plate with mass

diffusion, radiation absorption, hall and ion-slip currents has received much less attention. Hence, the main objective of the present investigation is to study the effects of viscous dissipative heat, radiation absorption, mass diffusion, Hall and ion-slip currents on the flow of a viscous incompressible heat generating fluid past an impulsively started vertical infinite porous plate subjected to constant suction and a strong transverse magnetic field.

2.0 MATHEMATICAL ANALYSIS

We consider free convection flow of an electrically conducting viscous incompressible fluid past an impulsively started vertical infinite porous plate subjected to constant suction velocity. The y^+ axis is taken along the plate in the vertically upward direction and x^+ axis is taken normal to the plate. A uniform transverse magnetic field H_0 is imposed along x^+ axis and the plate is taken to be electrically non-conducting. A second material is injected or exists in the main flow. This second material is a strong radiation absorbent, absorption rate being proportional to its concentration. At time $t^+ > 0$, the plate starts moving impulsively in its own plane with velocity U and its temperature is instantaneously raised or lowered to T_w^+ , which is maintained constant there after. The flow occurs at a low Mach number and hence the density of the ionised gas can be taken as constant. However, for such a fluid, the Hall and the ion-slip currents will significantly affect the flow in the presence of large magnetic fields. Since magnetic Reynolds number of a partially ionised fluid is very small, the induced magnetic field is negligible thus $\mathbf{H} = (H_0, 0, 0)$. The equation of conservation of electric charge is $\nabla \cdot \mathbf{J} = 0$ gives $j_{x^+} = \text{constant}$, $\mathbf{J} = (j_{x^+}, j_{y^+}, j_{z^+})$. As the plate is assumed to be electrically non-conducting, $j_{x^+} = 0$ at the plate. Thus $j_{x^+} = 0$ every where in the flow field. Since the plate is of infinite extent, along y^+ and z^+ directions, all the physical variables except pressure will be functions of x^+ and t^+ only.

The generalised ohm's law, Cowling [3] including Hall and ion-slip currents is written as

$$\mathbf{J} = \frac{\sigma}{1 + \left(\frac{\omega}{\nu_e}\right)^2} \left[\mathbf{E} + \mu_e \mathbf{q} \times \mathbf{H} - \mu_e \frac{\mathbf{J} \times \mathbf{B}}{\eta_e e} + \frac{1}{\eta_e e} \nabla p_e \right] \dots\dots\dots 1$$

For a short circuit problem, the applied electric field $\mathbf{E} = 0$ and for a slightly ionized gas the electron pressure gradient is negligible.

Thus equation (1) reduces to

$$\mathbf{J} = \frac{\sigma}{1 + \left(\frac{\omega}{\nu_c}\right)^2} \left[\mu_e \mathbf{q} \times \mathbf{H} - \mu_e \frac{\mathbf{J} \times \mathbf{B}}{\eta_e e} \right] \dots\dots\dots 2$$

Solving the above equation for the current density components j_{y^+} and j_{z^+} we have

$$j_{y^+} = \sigma H_o \mu_e (\alpha v^+ + \gamma w^+) \dots\dots\dots 3$$

$$j_{z^+} = \sigma H_o \mu_e (\alpha w^+ - \gamma v^+) \dots\dots\dots 4$$

where $\alpha = m / [(1 + mn)^2 + m^2]$ and $\gamma = (1 + mn) / [(1 + mn)^2 + m^2]$

$m = \omega_e \tau_e$ (Hall parameter)

$n = \omega_i \tau_i$ (ion-slip parameter)

Thus, under the usual Boussinesq approximation, the problem is governed by the following set of equations:

$$\frac{\partial u^+}{\partial x^+} = 0 \dots\dots\dots 5$$

$$\frac{\partial v^+}{\partial t^+} + u^+ \frac{\partial v^+}{\partial x^+} = g\beta((T^+ - T_\infty^+) + g\beta^*(C^+ - C_\infty^+)) + \nu \frac{\partial^2 v^+}{\partial x^{+2}} + \frac{\mu_e^2 H_o^2 \sigma}{\rho} (\alpha w^+ - \gamma v^+) \dots\dots\dots 6$$

$$\frac{\partial w^+}{\partial t^+} + u^+ \frac{\partial w^+}{\partial x^+} = \nu \frac{\partial^2 w^+}{\partial x^{+2}} - \frac{\mu_e^2 H_o^2 \sigma}{\rho} (\alpha v^+ + \gamma w^+) \dots\dots\dots 7$$

$$\frac{\partial T^+}{\partial t^+} + u^+ \frac{\partial T^+}{\partial x^+} = \frac{k}{\rho C_p} \frac{\partial^2 T^+}{\partial x^{+2}} + \frac{Q^+}{\rho C_p} + Q_1^+ C^+ + \frac{\nu}{C_p} \left[\left(\frac{\partial v^+}{\partial x^+}\right)^2 + \left(\frac{\partial w^+}{\partial x^+}\right)^2 \right] \dots\dots\dots 8$$

$$\frac{\partial C^+}{\partial t^+} + u^+ \frac{\partial C^+}{\partial x^+} = D \frac{\partial^2 C^+}{\partial x^{+2}} \dots\dots\dots 9$$

The initial and boundary conditions are:

for $t^+ \leq 0$: $v^+(x^+, t^+) = 0, w^+(x^+, t^+) = 0, T^+(x^+, t^+) = T_\infty^+, C^+(x^+, t^+) = C_\infty^+$

for $t^+ > 0$: $v^+(0, t^+) = U, w^+(0, t^+) = 0, T^+(0, t^+) = T_w^+, C^+(0, t^+) = C_w^+$

$v^+(\infty, t^+) = 0, w^+(\infty, t^+) = 0, T^+(\infty, t^+) = T_\infty^+, C^+(\infty, t^+) = C_\infty^+$

The equation of continuity, (5) gives $u^+ = -u_o^+$, where u_o^+ is the constant suction velocity.

Thus, equations (6) to (9) become;

$$\frac{\partial v^+}{\partial t^+} - u_o^+ \frac{\partial v^+}{\partial x^+} = g\beta(T_w^+ - T_\infty^+) + g\beta^*(C^+ - C_\infty^+) + \nu \frac{\partial^2 v^+}{\partial x^{+2}} + \frac{\mu_e^2 H_o^2 \sigma}{\rho} (\alpha v^+ - \gamma^+) \dots\dots\dots 10$$

$$\frac{\partial w^+}{\partial t^+} - u_o^+ \frac{\partial w^+}{\partial x^+} = \nu \frac{\partial^2 w^+}{\partial x^{+2}} - \frac{\mu_e^2 H_o^2 \sigma}{\rho} (\alpha v^+ + \gamma w^+) \dots\dots\dots 11$$

$$\frac{\partial T^+}{\partial t^+} - u_o^+ \frac{\partial T^+}{\partial x^+} = \frac{k}{\rho C_p} \frac{\partial^2 T^+}{\partial x^{+2}} + \frac{Q^+}{\rho C_p} + Q_1^+ C^+ + \frac{\nu}{C_p} \left[\left(\frac{\partial v^+}{\partial x^+} \right)^2 + \left(\frac{\partial w^+}{\partial x^+} \right)^2 \right] \dots\dots\dots 12$$

$$\frac{\partial C^+}{\partial t^+} - u_o^+ \frac{\partial C^+}{\partial x^+} = D \frac{\partial^2 C^+}{\partial x^{+2}} \dots\dots\dots 13$$

The internal heat generation is assumed to be of the form

$$Q^+ = -(T^+ - T_\infty^+)Q$$

On introducing the following dimensionless quantities,

$$x = \frac{x^+ U}{\nu}, \quad t = \frac{t^+ U^2}{\nu}, \quad v = \frac{v^+}{U}, \quad w = \frac{w^+}{U}, \quad u_o = \frac{u_o^+}{U}$$

$$P_r = \frac{\mu C_p}{k}, \quad G_r = \frac{\nu g \beta (T_w^+ - T_\infty^+)}{U^3}, \quad G_c = \frac{\nu g \beta^* (C_w^+ - C_\infty^+)}{U^3}$$

$$\delta = \frac{Q \nu}{K U^2}, \quad E_c = \frac{U^2}{C_p (T_w^+ - T_\infty^+)}, \quad M^2 = \frac{\sigma \mu_e^2 H_o^2 \nu}{\rho U^2}$$

$$C = \frac{C^+ - C_\infty^+}{C_w^+ - C_\infty^+}, \quad \theta = \frac{T^+ - T_\infty^+}{T_w^+ - T_\infty^+}, \quad s_c = \frac{D}{\nu}$$

Equations (10) to (13) become

$$\frac{\partial q}{\partial t} - u_o \frac{\partial q}{\partial x} = \frac{\partial^2 q}{\partial x^2} + G_r \theta + G_c C - M^2 \frac{[mi + (1 + mn)]}{(1 + mn)^2 + m^2} q \dots\dots\dots 14$$

$$\frac{\partial \theta}{\partial t} - u_o \frac{\partial \theta}{\partial x} = \frac{1}{P_r} \frac{\partial^2 \theta}{\partial x^2} - \frac{\delta}{P_r} \theta + Q_1 C + E_c \left(\frac{\partial q}{\partial x} \frac{\partial \bar{q}}{\partial x} \right) \dots\dots\dots 15$$

$$\frac{\partial C}{\partial t} - u_o \frac{\partial C}{\partial x} = S_c \frac{\partial^2 C}{\partial x^2} \dots\dots\dots 16$$

where, $q = v + iw$ is the complex velocity and \bar{q} denotes the complex conjugate of q .

The non-dimensional form of the initial and boundary conditions are:

$$t \leq 0 \quad : \quad q(x,0) = 0, \quad \theta(x,0) = 0, \quad C(x,0) = 0 \dots\dots\dots 17a$$

$$t > 0 \quad : \quad q(0,t) = 1, \quad \theta(0,t) = 1, \quad C(0,t) = 1 \dots\dots\dots 17b$$

$$q(\infty, t) = 0, \theta(\infty, t) = 0, C(\infty, t) = 0 \dots\dots\dots 17c$$

2.1 Solution of the Problem by Explicit Finite-Difference Method

To solve equations (14) to (16) subject to the initial and boundary conditions (17a) and (17c) we apply the finite difference method, since the exact solution of these non-linear equations is not possible. The following algorithm is employed.

$$\frac{q(i, j+1) - q(i, j)}{\Delta t} = u_o \frac{[q(i, j) - q(i-1, j)]}{\Delta x} + \frac{[q(i-1, j) - 2q(i, j) + q(i+1, j)]}{(\Delta x)^2} + G_r \theta(i, j) + G_c C(i, j) - M^2 \frac{[mi + (1 + mn)]}{(1 + mn)^2 + m^2} q(i, j) \dots\dots\dots 18$$

$$\frac{\theta(i, j+1) - \theta(i, j)}{\Delta t} = u_o \frac{[\theta(i, j) - \theta(i-1, j)]}{\Delta x} + \frac{[\theta(i-1, j) - 2\theta(i, j) + \theta(i+1, j)]}{P_r (\Delta x)^2} - \frac{\delta}{P_r} \theta(i, j) + Q_1 C(i, j) + E_c \left(\frac{q(i, j) - q(i-1, j)}{\Delta x} \right) \left(\frac{\bar{q}(i, j) - \bar{q}(i-1, j)}{\Delta x} \right) \dots\dots\dots 19$$

$$\frac{C(i, j+1) - C(i, j)}{\Delta t} = u_o \frac{[C(i, j) - C(i-1, j)]}{\Delta x} + s_c \frac{[C(i-1, j) - 2C(i, j) + C(i+1, j)]}{(\Delta x)^2} \dots\dots\dots 20$$

The index i refers to x and j to t. Δx is taken as 0.1 and Δt as 0.0012. From (17a), the initial conditions at x = 0 in finite difference take the form

$$q(0,0) = 1, \theta(0,0) = 1, C(0,0) = 1$$

$$q(i,0) = 0, \theta(i,0) = 0, C(i,0) = 0 \text{ for all } i \text{ except } i=0$$

The boundary conditions (17b) take the form

$$q(0, j) = 1, \theta(0, j) = 1, C(0, j) = 1 \text{ for all } j$$

The boundary conditions (17c) which applies to x = ∞ corresponds to i=51 [i.e. q(51,,j)= θ(51, j)=C (51, j)=0] This is because q, θ and C tend to zero at around x=5. The velocity at the end of time-step i.e. q(i,j+1), i=1,2, ----- 50 is computed from (18) in terms of velocities, temperatures and concentrations at points on the earlier time-step. Similarly θ(i, j + 1) and C(i, j + 1) are computed from equations 19 and 20 respectively. The procedure is repeated until j=350, i.e. up to time t=0.42. To ensure the convergence and stability of the finite difference scheme, the computations were done with smaller values of Δt=0.0007, 0.0009 and there were no significant changes in the results. Hence the finite difference scheme followed in the present analysis converges and is stable.

Skin frictions τ_y , τ_z , the rate of mass transfer s_h and the rate of heat transfer N_u were calculated from the velocity, concentration and temperature profiles by using the equations

$$\tau_y = -\frac{\partial v}{\partial x} \Big|_{x=0}, \quad \tau_z = -\frac{\partial w}{\partial x} \Big|_{x=0}, \quad s_h = -\frac{\partial c}{\partial x} \Big|_{x=0}$$

$$\text{and } N_u = -\frac{\partial \theta}{\partial x} \Big|_{x=0}$$

To determine the above gradients, a second order-least squares correlation was used over the first twelve points.

3.0 RESULTS (DISCUSSION AND CONCLUSIONS)

The dimensionless concentration profiles, velocity profiles and temperature profiles for different values of the Eckert number, $E_c = 0.01$ and $E_c = 0.03$ are shown in figures 1 to 7.

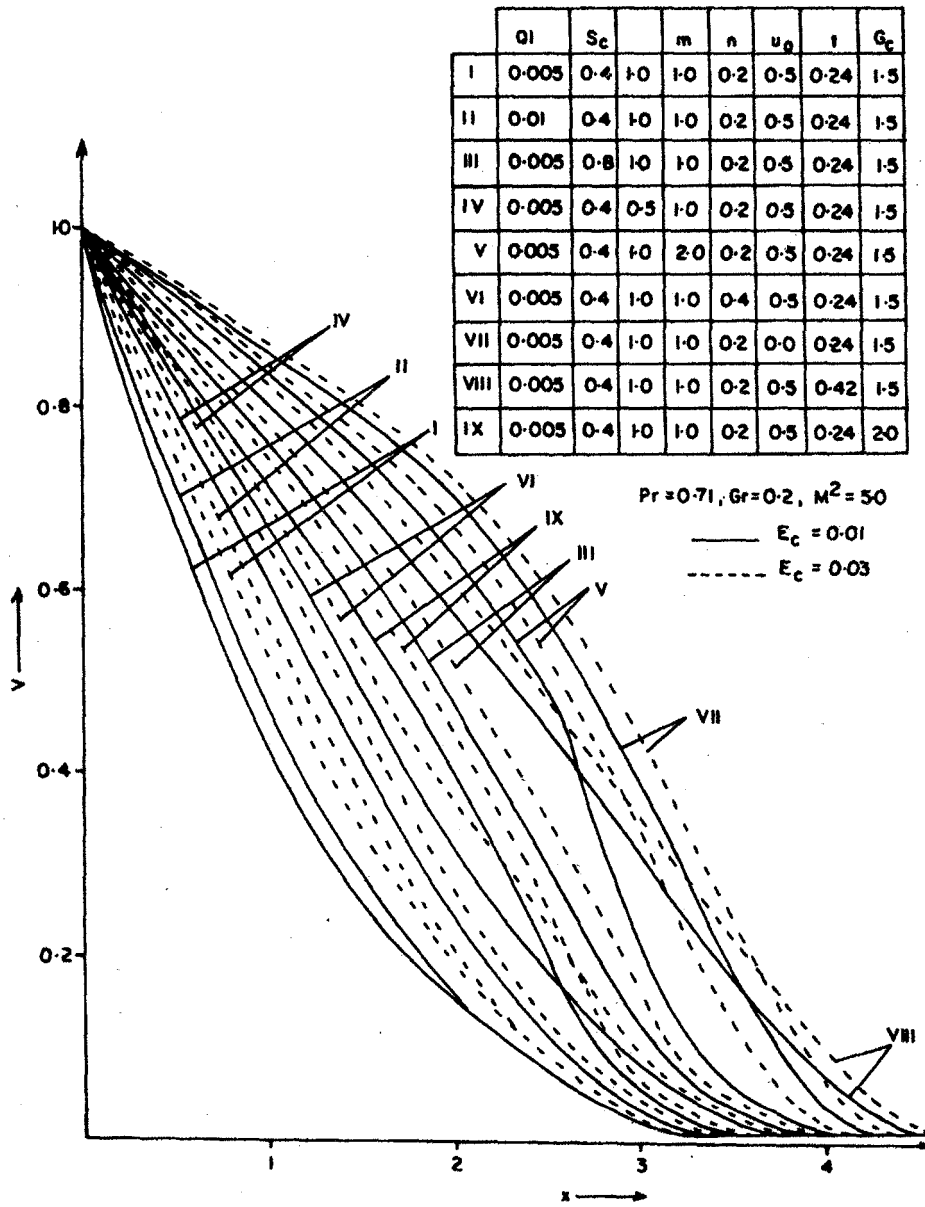


Fig. 1: Primary velocity profiles V

	Q_1	S_c		m	n	u_0	t	G_c
I	0.005	0.4	1.0	1.0	0.2	0.5	0.24	1.5
II	0.01	0.4	1.0	1.0	0.2	0.5	0.24	1.5
III	0.005	0.8	1.0	1.0	0.2	0.5	0.24	1.5
IV	0.005	0.4	0.5	1.0	0.2	0.5	0.24	1.5
V	0.005	0.4	1.0	2.0	0.2	0.5	0.24	1.5
VI	0.005	0.4	1.0	1.0	0.4	0.5	0.24	1.5
VII	0.005	0.4	1.0	1.0	0.2	0.0	0.24	1.5
VIII	0.005	0.4	1.0	1.0	0.2	0.5	0.42	1.5
IX	0.005	0.4	1.0	1.0	0.2	0.5	0.24	2.0

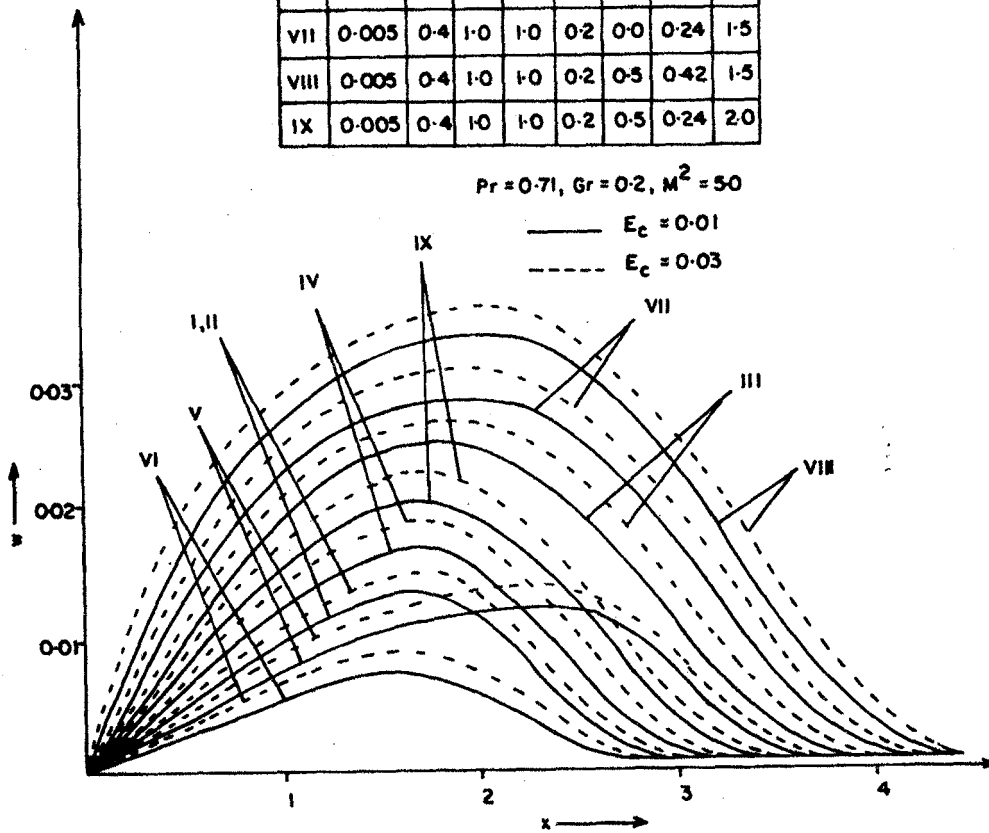


Fig. 2 : Secondary velocity profiles w

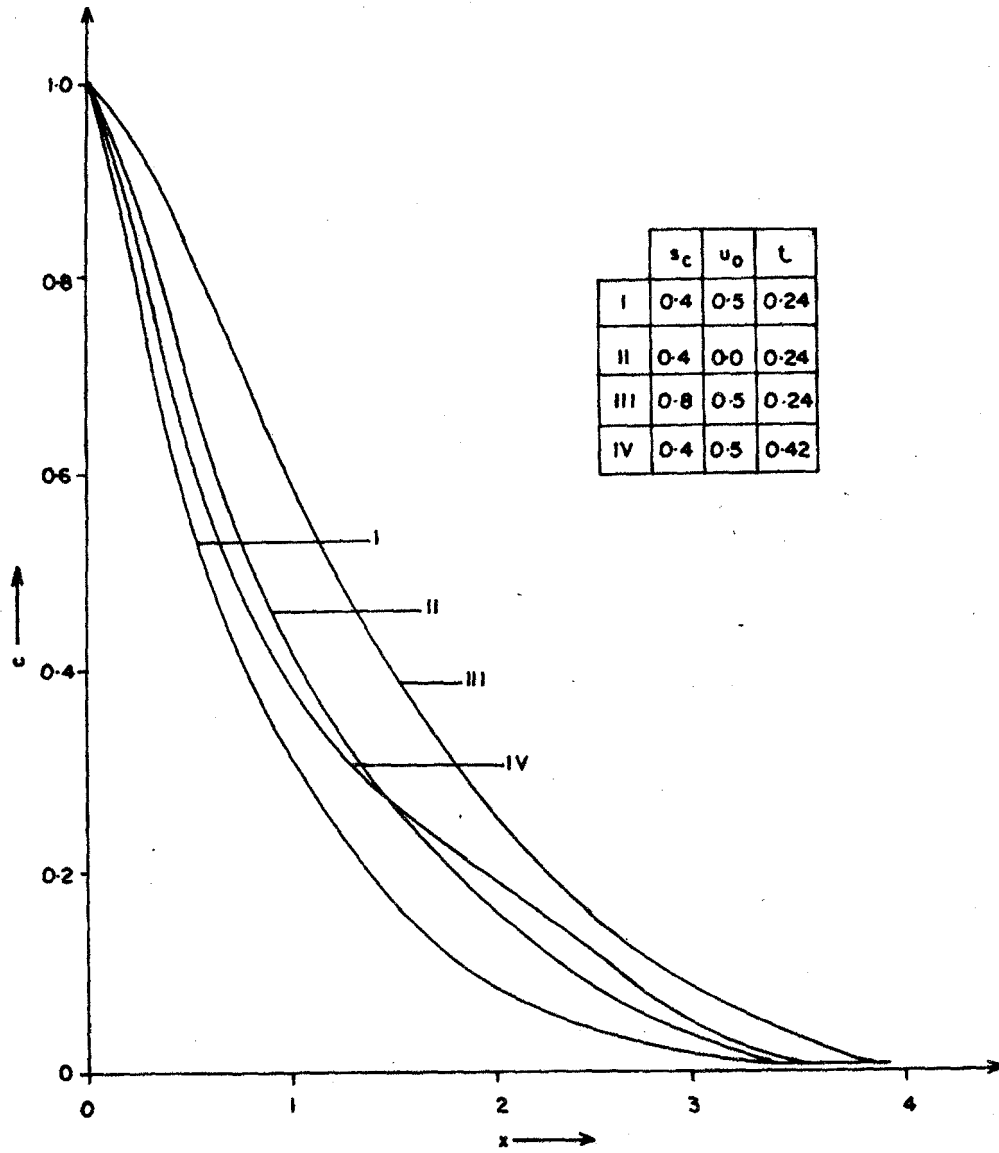


Fig. 3: Concentration profiles c

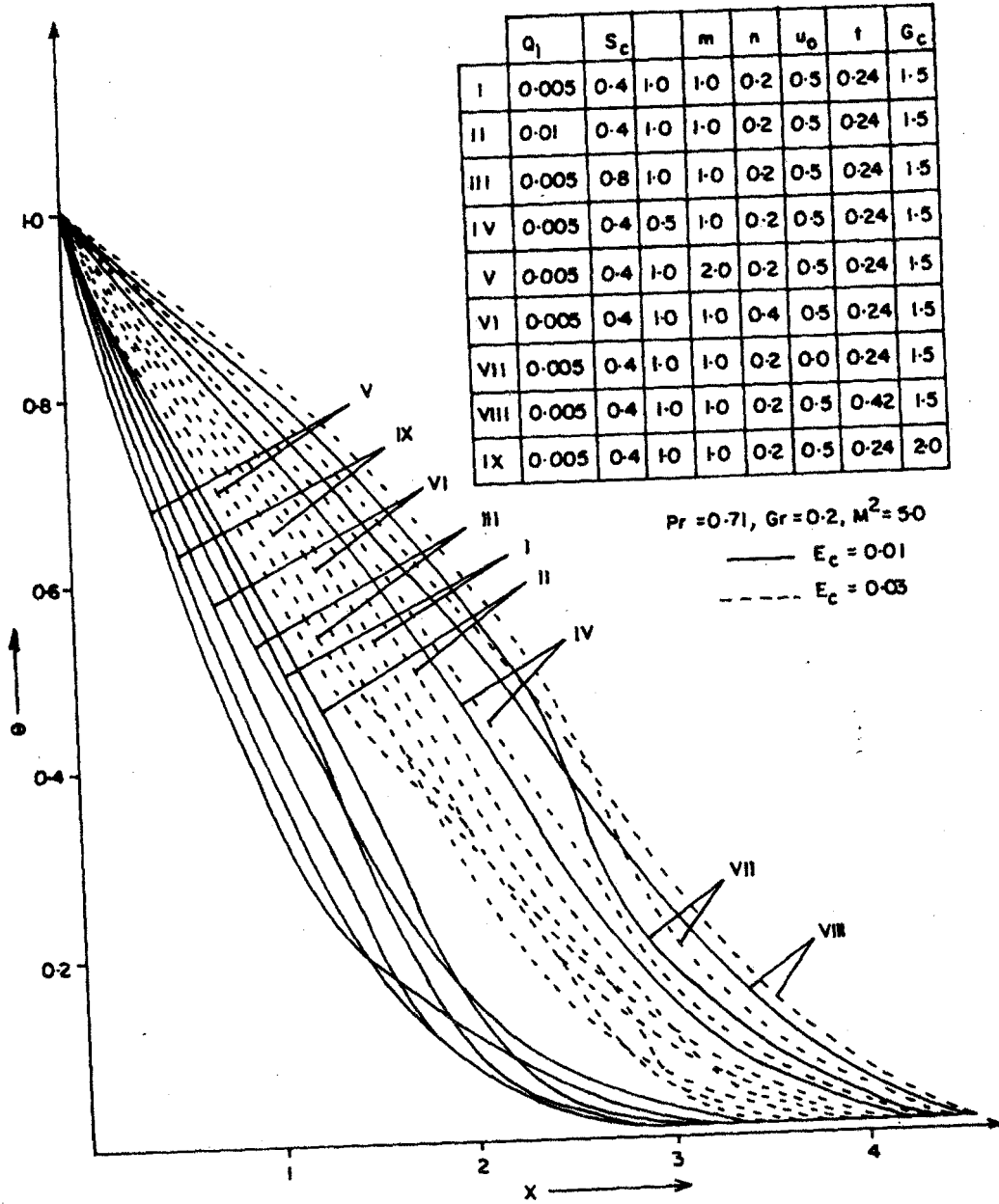


Fig. 4: Temperature profiles θ

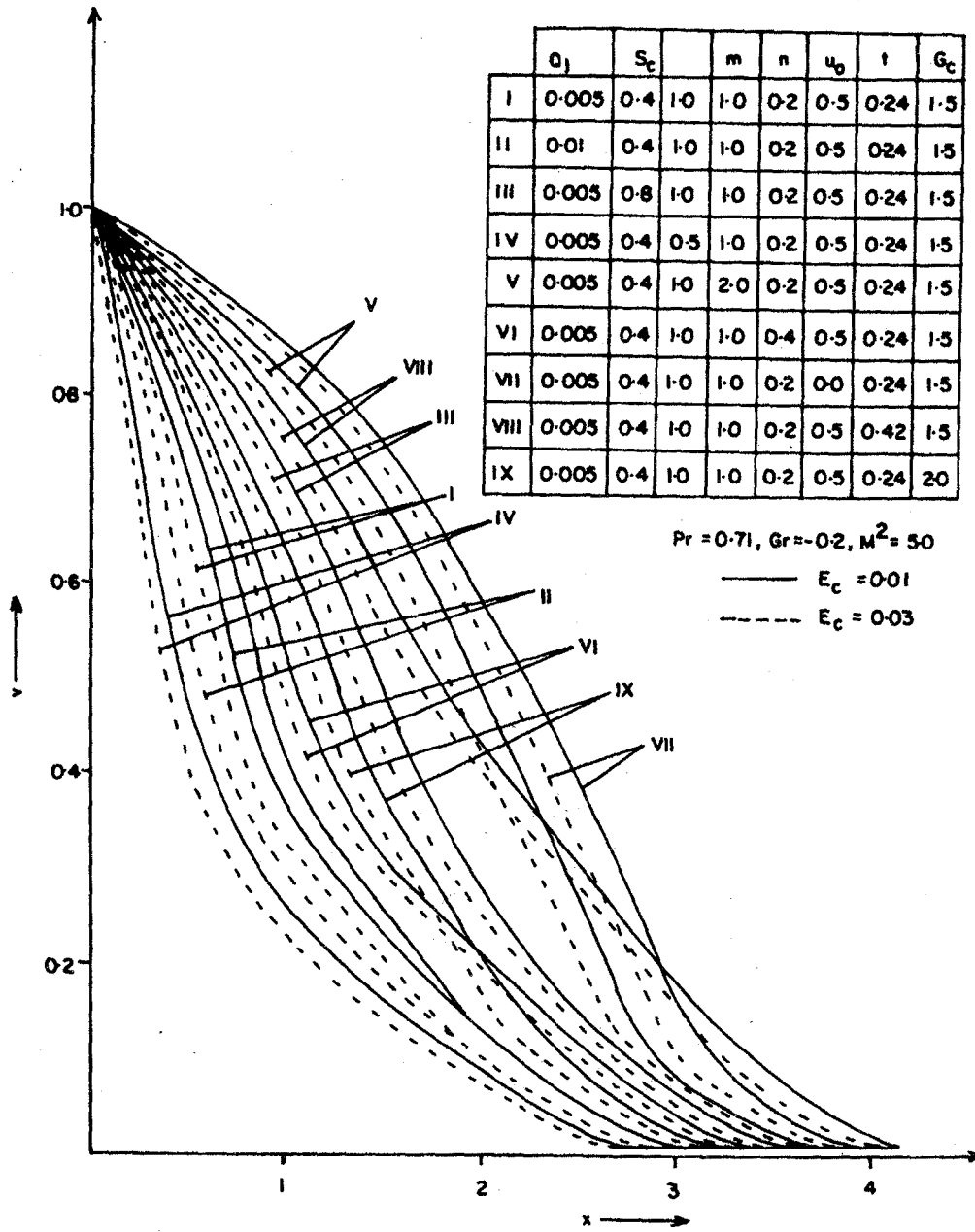


Fig. 5: Primary velocity profiles v

	Q_1	S_c		m	n	u_0	t	G_c
I	0.005	0.4	1.0	1.0	0.2	0.5	0.24	1.5
II	0.01	0.4	1.0	1.0	0.2	0.5	0.24	1.5
III	0.005	0.8	1.0	1.0	0.2	0.5	0.24	1.5
IV	0.005	0.4	0.5	1.0	0.2	0.5	0.24	1.5
V	0.005	0.4	1.0	2.0	0.2	0.5	0.24	1.5
VI	0.005	0.4	1.0	1.0	0.4	0.5	0.24	1.5
VII	0.005	0.4	1.0	1.0	0.2	0.0	0.24	1.5
VIII	0.005	0.4	1.0	1.0	0.2	0.5	0.42	1.5
IX	0.005	0.4	1.0	1.0	0.2	0.5	0.24	2.0

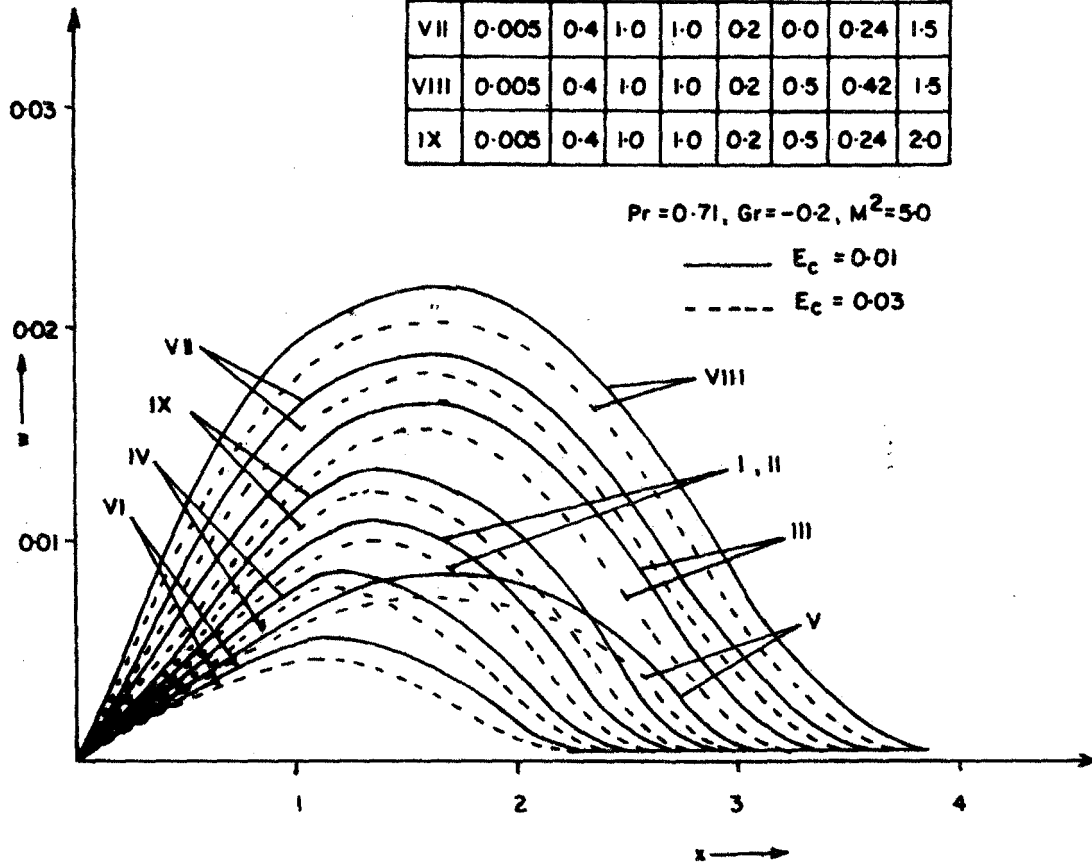


Fig. 6: Secondary velocity profiles w

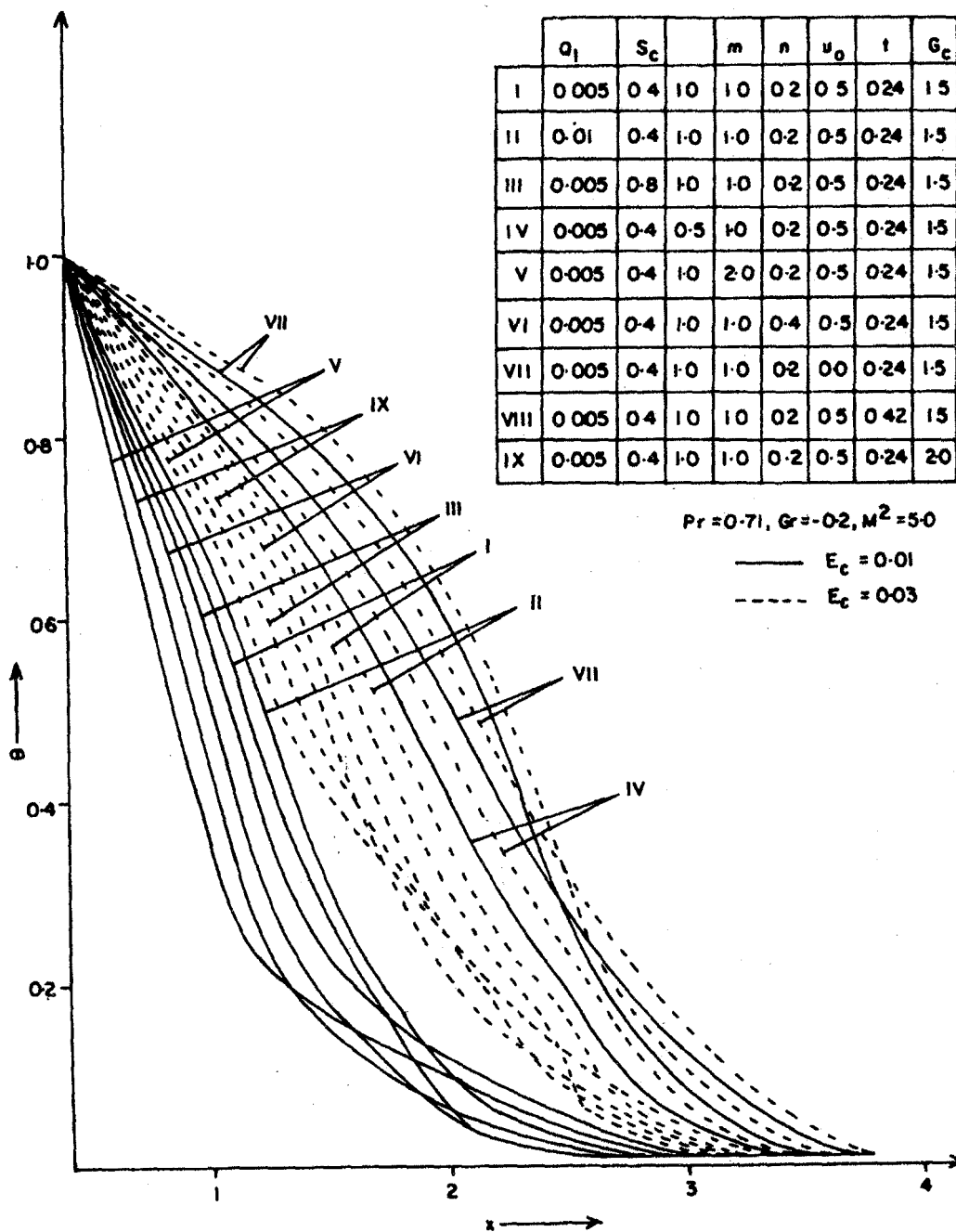


Fig.7 : Temperature velocity profiles θ

These values of Eckert number where chosen because for incompressible viscous fluid $E_c \ll 1$. Skin friction τ , the rate of mass transfer s_h and the rate of heat transfer N_u for $E_c = 0.01$ and $E_c = 0.03$ are shown in tables 1 to 9.

Table 1

$G_r = 0.2, E_c = 0.01, P_r = 0.71, M^2 = 5.0$

Q_1	s_c	δ	m	n	u_0	t	G_c	τ_y	τ_z
0.005	0.4	1.0	1.0	0.2	0.5	0.05	1.5	2.427619	0.4877915
0.01	0.4	1.0	1.0	0.2	0.5	0.05	1.5	2.42762	0.4877921
0.005	0.8	1.0	1.0	0.2	0.5	0.05	1.5	2.29135	0.5079593
0.005	0.4	0.5	1.0	0.2	0.5	0.05	1.5	2.424787	0.4873647
0.005	0.4	1.0	2.0	0.2	0.5	0.05	1.5	2.042842	0.4931739
0.005	0.4	1.0	1.0	0.4	0.5	0.05	1.5	2.373094	0.4090023
0.005	0.4	1.0	1.0	0.2	0.0	0.05	1.5	2.1999265	0.5437179
0.005	0.4	1.0	1.0	0.2	0.5	0.06	1.5	4.0970432	0.4926792
0.005	0.4	1.0	1.0	0.2	0.5	0.05	2.0	2.3549485	0.4999254

Table 2

$G_r = 0.2, E_c = 0.03, P_r = 0.71, M^2 = 5.0$

Q_1	s_c	δ	m	n	u_0	t	G_c	τ_y	τ_z
0.005	0.4	1.0	1.0	0.2	0.5	0.05	1.5	2.4274095	0.4878602
0.01	0.4	1.0	1.0	0.2	0.5	0.05	1.5	2.4273835	0.4882049
0.005	0.8	1.0	1.0	0.2	0.5	0.05	1.5	2.2911415	0.5080301
0.005	0.4	0.5	1.0	0.2	0.5	0.05	1.5	2.424563787	0.4874133
0.005	0.4	1.0	2.0	0.2	0.5	0.05	1.5	2.042629	0.4931718
0.005	0.4	1.0	1.0	0.4	0.5	0.05	1.5	2.3729015	0.4090448
0.005	0.4	1.0	1.0	0.2	0.0	0.05	1.5	2.199719	0.5437664
0.005	0.4	1.0	1.0	0.2	0.5	0.06	1.5	4.0968244	0.4927755
0.005	0.4	1.0	1.0	0.2	0.5	0.05	2.0	2.354713	0.4999832

Table 3

s_c	u_0	t	S_h
0.4	0.5	0.05	2.579066
0.8	0.5	0.05	2.1512395
0.4	0.0	0.05	2.288725
0.4	0.5	0.06	4.4981898

Table 4

$E_c = 0.01, M^2 = 5.0, G_r = 0.2, P_r = 0.71$

Q_1	s_c	δ	m	n	u_0	t	G_c	N_u
0.005	0.4	1.0	1.0	0.2	0.5	0.05	1.5	2.038335
0.01	0.4	1.0	1.0	0.2	0.5	0.05	1.5	2.0377105
0.005	0.8	1.0	1.0	0.2	0.5	0.05	1.5	2.038209
0.005	0.4	0.5	1.0	0.2	0.5	0.05	1.5	1.8580815
0.005	0.4	1.0	2.0	0.2	0.5	0.05	1.5	2.0386125
0.005	0.4	1.0	1.0	0.4	0.5	0.05	1.5	2.03845
0.005	0.4	1.0	1.0	0.2	0.0	0.05	1.5	1.8985895
0.005	0.4	1.0	1.0	0.2	0.5	0.06	1.5	3.4673432
0.005	0.4	1.0	1.0	0.2	0.5	0.05	2.0	2.0383115

Table 5

$E_c = 0.03, M^2 = 5.0, G_r = 0.2, P_r = 0.71$

Q_1	s_c	δ	m	n	u_0	t	G_c	N_u
0.005	0.4	1.0	1.0	0.2	0.5	0.05	1.5	2.025857
0.01	0.4	1.0	1.0	0.2	0.5	0.05	1.5	2.0252355
0.005	0.8	1.0	1.0	0.2	0.5	0.05	1.5	2.026227
0.005	0.4	0.5	1.0	0.2	0.5	0.05	1.5	1.844923
0.005	0.4	1.0	2.0	0.2	0.5	0.05	1.5	2.026784
0.005	0.4	1.0	1.0	0.4	0.5	0.05	1.5	2.026218
0.005	0.4	1.0	1.0	0.2	0.0	0.05	1.5	1.886399
0.005	0.4	1.0	1.0	0.2	0.5	0.06	1.5	3.4430356
0.005	0.4	1.0	1.0	0.2	0.5	0.05	2.0	2.0258225

Table 6

$G_r = 0.2, E_c = 0.01, P_r = 0.71, M^2 = 5.0,$

Q_1	s_c	δ	m	n	u_0	t	G_c	τ_y	τ_z
0.005	0.4	1.0	1.0	0.2	0.5	0.05	1.5	2.541918	0.4653195
0.01	0.4	1.0	1.0	0.2	0.5	0.05	1.5	2.541927	0.4653283
0.005	0.8	1.0	1.0	0.2	0.5	0.05	1.5	2.4056695	0.4854989
0.005	0.4	0.5	1.0	0.2	0.5	0.05	1.5	2.544767	0.4657627
0.005	0.4	1.0	2.0	0.2	0.5	0.05	1.5	2.1717675	0.477797
0.005	0.4	1.0	1.0	0.4	0.5	0.05	1.5	2.4882785	0.3909054
0.005	0.4	1.0	1.0	0.2	0.0	0.05	1.5	2.3213065	0.5229555
0.005	0.4	1.0	1.0	0.2	0.5	0.06	1.5	4.2147454	0.462382
0.005	0.4	1.0	1.0	0.2	0.5	0.05	2.0	2.469246	0.4774464

Table 7

$G_r = 0.2, E_c = 0.03, P_r = 0.71 M^2 = 5.0$

Q_1	s_c	δ	m	n	u_0	t	G_c	τ_y	τ_z
0.005	0.4	1.0	1.0	0.2	0.5	0.05	1.5	2.542153	0.4653195
0.01	0.4	1.0	1.0	0.2	0.5	0.05	1.5	2.541525	0.4653283
0.005	0.8	1.0	1.0	0.2	0.5	0.05	1.5	2.4058705	0.4854989
0.005	0.4	0.5	1.0	0.2	0.5	0.05	1.5	2.545016	0.4657627
0.005	0.4	1.0	2.0	0.2	0.5	0.05	1.5	2.1719765	0.477797
0.005	0.4	1.0	1.0	0.4	0.5	0.05	1.5	2.4884885	0.3909054
0.005	0.4	1.0	1.0	0.2	0.0	0.05	1.5	2.321527	0.5229555
0.005	0.4	1.0	1.0	0.2	0.5	0.06	1.5	4.21499	0.462382
0.005	0.4	1.0	1.0	0.2	0.5	0.05	2.0	2.469457	0.4774464

Table 8

$G_r = 0.2, E_c = 0.01, P_r = 0.71 M^2 = 5.0,$

Q_1	s_c	δ	m	n	u_0	t	G_c	N_u
0.005	0.4	1.0	1.0	0.2	0.5	0.05	1.5	2.038219
0.01	0.4	1.0	1.0	0.2	0.5	0.05	1.5	2.0376075
0.005	0.8	1.0	1.0	0.2	0.5	0.05	1.5	2.0381125
0.005	0.4	0.5	1.0	0.2	0.5	0.05	1.5	1.857955
0.005	0.4	1.0	2.0	0.2	0.5	0.05	1.5	2.038545
0.005	0.4	1.0	1.0	0.4	0.5	0.05	1.5	2.0383225
0.005	0.4	1.0	1.0	0.2	0.0	0.05	1.5	1.898434
0.005	0.4	1.0	1.0	0.2	0.5	0.06	1.5	3.4672726
0.005	0.4	1.0	1.0	0.2	0.5	0.05	2.0	2.038214

Table 9

$G_r = 0.2, E_c = 0.03, P_r = 0.71 M^2 = 5.0,$

Q_1	s_c	δ	m	n	u_0	t	G_c	N_u
0.005	0.4	1.0	1.0	0.2	0.5	0.05	1.5	2.025499
0.01	0.4	1.0	1.0	0.2	0.5	0.05	1.5	2.0249
0.005	0.8	1.0	1.0	0.2	0.5	0.05	1.5	2.0259305
0.005	0.4	0.5	1.0	0.2	0.5	0.05	1.5	1.844496
0.005	0.4	1.0	2.0	0.2	0.5	0.05	1.5	2.026442
0.005	0.4	1.0	1.0	0.4	0.5	0.05	1.5	2.0258735
0.005	0.4	1.0	1.0	0.2	0.0	0.05	1.5	1.885961
0.005	0.4	1.0	1.0	0.2	0.5	0.06	1.5	3.4428022
0.005	0.4	1.0	1.0	0.2	0.5	0.05	2.0	2.0255125

M^2 is chosen arbitrarily to be equal to 5.0 which signifies strong magnetic field. $G_r < 0 (= -0.2)$ corresponds to heating of the plate by free convection currents while

$G_r > 0 (= 0.2)$ corresponds to cooling of the plate by free convection currents.

Prandtl number $P_r = 0.71$ corresponds to air.

From Figures 1 and 2 we observe that:

- (i) An increase in radiation absorption parameter Q_1 leads to an increase in primary velocity profiles for both $E_c = 0.01$ and $E_c = 0.03$ but as the distance from the plate increases it has no effect. Q_1 has no effect on secondary velocity profile.
- (ii) As the mass diffusion parameter s_c increases the primary and secondary velocity profiles also increase for both $E_c = 0.01$ and $E_c = 0.03$.
- (iii) For both $E_c = 0.01$ and $E_c = 0.03$ increase in Hall parameter m leads to an increase in primary velocity profile but causes a decrease in secondary velocity profile. However, it is noted that as the distance from the plate increases, increase in Hall parameter m leads to an increase in secondary velocity profile.
- (iv) An increase in ionslip current parameter n leads to an increase in primary velocity profile but causes a decrease in secondary velocity profile for both $E_c = 0.01$ and $E_c = 0.03$.
- (v) A decrease in heat source parameter δ or removal of suction velocity u_0 leads to an increase in both primary and secondary velocity profiles for both $E_c = 0.01$ and $E_c = 0.03$.
- (vi) Increase in time t or modified Grashof number G_c causes an increase in both primary and secondary velocity profiles for both $E_c = 0.01$ and $E_c = 0.03$

In all cases the velocity profiles for $E_c = 0.01$ are lower than the corresponding velocity profiles for $E_c = 0.03$. This leads us to the conclusion that in presence of cooling of plate by free convection currents ($G_r > 0$) increase in viscous dissipative heat causes an increase in the velocity boundary layer thickness.

From Figure 3 we note that:

- (i) Increase in mass diffusion parameter s_c or increase in time t leads to an increase in concentration profile.
- (ii) In the absence of suction velocity u_0 the concentration profile increases.

From Figure 4 we note that:

- (i) A rise in radiation absorption parameter Q_1 leads to an increase in temperature profile for both $E_c = 0.01$ and $E_c = 0.03$.
- (ii) Increase in mass diffusion parameter s_c leads to a fall in temperature profile for both $E_c = 0.01$ and $E_c = 0.03$.
- (iii) A fall in heat source parameter δ causes a rise in temperature profile for the two cases of viscous dissipative heat parameters $E_c = 0.01$ and $E_c = 0.03$.
- (iv) For $E_c = 0.01$ and $E_c = 0.03$, increase in ion-slip current parameter n or Hall parameter m leads to a fall in temperature profile.
- (v) As the modified Grashof number G_c increases the temperature profile decreases for both $E_c = 0.01$ and $E_c = 0.03$.
- (vi) Withdrawal of suction velocity u_0 or increase in time t leads to an increase in temperature profile for both $E_c = 0.01$ and $E_c = 0.03$.

In all cases temperature profiles for $E_c = 0.03$ are higher than those for $E_c = 0.01$. This shows that increase in viscous dissipative heat leads to an increase in thermal boundary layer thickness.

From Figures 5 and 6 we note that:

- (i) For both $E_c = 0.01$ and $E_c = 0.03$, an increase in radiation absorption parameter Q leads to a decrease in primary velocity profile. However, as the distance from the plate increases it has no effect on primary velocity profile. An increase in radiation absorption parameter Q_1 has no impact on secondary velocity profile for both $E_c = 0.01$ and $E_c = 0.03$.
- (ii) As the heat source parameter δ decreases, both primary and secondary velocity profiles decrease for $E_c = 0.01$ and $E_c = 0.03$.
- (iii) Increase in mass diffusion parameter s_c or modified Grashof number G_c causes an increase in both primary and secondary velocity profiles for $E_c = 0.01$ and $E_c = 0.03$.
- (iv) An increase in Hall current parameter m or ion-slip current parameter n leads to an increase in primary velocity profile but causes a decrease in secondary velocity profile for both $E_c = 0.01$ and $E_c = 0.03$.
- (v) Withdrawal for suction velocity u_0 or increase in time t leads to a rise in both primary and secondary velocity profiles.

We note that the trends of temperature profiles in Figure 7 are the same as in those in Figure 4. For these figures the values of Gr are 0.2 and -0.2 . The governing equations were also solved taking $Gr = 10$ and $Gr = -10$ and it was found that there was no change in the trends of the temperature profiles. It is noted that the temperature profiles in Figure 4 are slightly higher than those in Figure 7 which leads us to the deduction that a change in Grashof number has very little impact on temperature profiles. Also, from these two Figures we conclude that heating of the plate by free convection currents leads to a slight decrease in thermal boundary layer thickness.

From Tables 1 and 2 we observe that:

- (i) An increase in radiation absorption parameter Q_1 leads to a slight increase in skin friction
- (ii) τ_y due to primary velocity for $E_c = 0.01$ but causes a slight decrease for $E_c = 0.03$. However, increase in Q_1 causes an increase in skin friction τ_z due to secondary velocity for both $E_c = 0.01$ and $E_c = 0.03$
- (iii) As the mass diffusion parameter s_c increases, skin friction τ_z due to secondary velocity for both $E_c = 0.01$ and $E_c = 0.03$ increases but skin friction τ_y due to primary velocity decreases.
- (iv) Both skin frictions τ_y due to primary velocity and skin friction τ_z due to secondary velocity decrease as the heat source parameter δ decreases for both $E_c = 0.01$ and $E_c = 0.03$
- (v) An increase in Hall current parameter m , removal of suction velocity u_0 or increase in modified Grashof number G_c leads to a decrease in skin friction τ_y due to primary velocity but causes an increase in skin friction τ_z due to secondary velocity for both $E_c = 0.01$ and $E_c = 0.03$
- (vi) For both $E_c = 0.01$ and $E_c = 0.03$, increase in ion-slip current parameter n leads to a fall in both skin friction τ_y due to primary velocity and skin friction τ_z due to secondary velocity.
- (vii) As time t increases skin friction τ_y due to primary velocity and skin friction τ_z due to secondary velocity increases for both $E_c = 0.01$ and $E_c = 0.03$

From Table 3 we note that:

- (i) In the absence of suction velocity u_0 , the rate of convection mass transfer s_h at the plate decreases
- (ii) As the mass diffusion parameter S_c increases the rate of convection mass transfer s_h at the plate decreases.
- (iii) Increase in time t leads to an increase in the rate of convection mass transfer s_h at the plate

From Tables 4 and 5 we observe that:

- (i) As the radiation absorption parameter Q_1 increases the rate of convection heat transfer N_u at the plate decreases for both $E_c = 0.01$ and $E_c = 0.03$
- (ii) Increase in mass diffusion parameter s_c Hall current parameter m or ion-slip current parameter n leads to an increase in the rate of convection heat transfer N_u at the plate for both $E_c = 0.01$ and $E_c = 0.03$
- (iii) A decrease in heat source parameter δ or withdrawal of suction velocity u_0 causes a decrease in the rate of free convection heat transfer N_u at the plate for both $E_c = 0.01$ and $E_c = 0.03$
- (iv) For both $E_c = 0.01$ and $E_c = 0.03$, the rate of convection heat transfer N_u at the plate decreases as the modified Grashof number G_c increases.
- (v) A decrease in heat source parameter δ or withdrawal of suction velocity u_0 causes a fall in the rate of free convection heat transfer N_u at the plate for both $E_c = 0.01$ and $E_c = 0.03$

From Tables 6 and 7, we observe that:

- (i) Increase in radiation absorption parameter Q_1 leads to a slight increase in both skin friction τ_y due to primary velocity and skin friction τ_z due to secondary velocity for $E_c = 0.01$. However, for $E_c = 0.03$ increase in Q_1 leads to a decrease in both τ_y and τ_z .
- (ii) As the mass diffusion parameter s_c increases skin friction τ_y due to primary velocity decreases for both $E_c = 0.01$ and $E_c = 0.03$. However skin friction τ_z due to secondary velocity increases for both $E_c = 0.01$ and $E_c = 0.03$
- (iii) A decrease in heat source parameter δ leads to an increase in both skin friction τ_y due to primary velocity and skin friction τ_z due to secondary velocity for both $E_c = 0.01$ and $E_c = 0.03$

- (iv) A rise in Hall current parameter m or modified Grashof number G_c leads to a fall in skin friction τ_y due to primary velocity but causes a rise in skin friction τ_z due to secondary velocity for both $E_c = 0.01$ and $E_c = 0.03$
- (v) Increase in ion-slip current parameter n causes a fall in skin friction τ_y due to primary velocity and skin friction τ_z due to secondary velocity for both $E_c = 0.01$ and $E_c = 0.03$
- (vi) As time t increases skin friction τ_y due to primary velocity increases for both cases of $E_c = 0.01$ and $E_c = 0.03$ but skin friction τ_z due to secondary velocity decreases for the two cases.
- (vii) Absence of suction velocity u_0 leads to a fall in skin friction τ_y due to primary velocity but causes an increase in skin friction τ_z due to secondary velocity.

From Tables 8 and 9 we note that the trends of the rate s of convection heat transfer N_u is the same as for Tables 4 and 5. However, the values of N_u in Tables 4 and 5 are higher than their corresponding values in Tables 8 and 9. This shows that the rate of convection heat transfer is higher for $G_r > 0$ ($= 0.2$ corresponding to cooling of the plate by free convection currents) than for $G_r < 0$ ($= -0.2$ corresponding to heating of the plate by free convection currents).

Generally from Tables 1, 2, 6 and 7, it is seen that the values of skin friction τ_y due to primary velocity in Tables 6 and 7 ($G_r < 0$) are higher than their corresponding values in Tables 1 and 2 ($G_r > 0$). This implies that skin friction τ_y due to primary velocity is more in presence of heating of the plate by free convection currents than in presence of cooling of the plate by free convection currents. The values of skin friction τ_z due to secondary velocity in Tables 1 and 2 are higher than those in Tables 6 and 7. This shows that skin friction τ_z due to secondary velocity is higher in presence of cooling of plate by free convection currents ($G_r > 0$) than in presence of heating of the plate by free convection currents ($G_r < 0$).

REFERENCES

- Bansal, J. L., Jat, R. N. and Nuouo Cimento D. (1987) Magnetohydrodynamic boundary layer flow in the presence of transverse magnetic field, *Proc. Indian Nat Sci. Acad. Part A*, 52, (6) 1398 – 1412
- Chaturvedi, N. (1987) Hydromagnetic flow past a uniformly started porous plate with constant suction, *Jour. Sci Res* 9 (2) and (3) 89 – 93.

- Cowling, T.G.(1957) Magnetohydrodynamics, Interscience, New-York.
- Dash, G.C. and Ojha, B.K (1990) Magnetohydrodynamics unsteady free convection effect on the flow past an exponentially accelerated vertical plate, *Model. Simul. Control B.* 27, (1) 1 – 10.
- Dash, G.C. and Tripathy, P.C. (1993): Convection heat and Mass transfer of a viscous flow past a hot vertical plane wall with periodic suction and heat sources, modelling, measurement and control B. 49, (1) 1 – 22.
- Hossain, M.A. and Rashid, R.I. (1987) Hall effects on hydromagnetic free convection flow along a porous flat plate with mass transfer. *J. Phys. Soc. Jpn*, 56, (1) 97 – 104.
- Kinyanjui , M., Charturvedi, N. and Uppal, S. M. (1998) MHD stokes problem for a vertical infinite plate in X a dissipative Rotating fluid with Hall Current, *Energy convers. Mgmt*, 39, (516) 541 – 548.
- Kinyanjui , M., Kwanza, J.K. and Uppal S. M.(2001): MHD free convection heat and mass transfer of a heat generating fluid past an impulsively started infinite vertical porous plate with Hall current and radiation absorption, *Energy convers. Mgmt*. 42, (8) 917 – 931.
- Lai, F.C (1990) Coupled heat and mass transfer by natural convection from a horizontal line source in a saturated porous medium, *Int. commun. Heat mass transfer*. 17, (4) 489 – 499.
- Ram P. C. (1991) Finite difference analysis of the MHD stokes problem for a vertical plate with Hall and ion-slip currents. *Astrophysics and space science* 176, 263 – 270.
- Schercliff J. A. (1965) *A text book on magnetohydrodynamics* Pergamon press: